

# Literature Report

---

**Reporter: Kang-Ming Xiong**

**Date: 2020-11-12**



pubs.acs.org/JACS

Article

## Photochromic Fluorescent Probe Strategy for the Super-resolution Imaging of Biologically Important Biomarkers

Xianzhi Chai,<sup>#</sup> Hai-Hao Han,<sup>#</sup> Adam C. Sedgwick,<sup>#</sup> Na Li, Yi Zang, Tony D. James, Junji Zhang,\*  
Xi-Le Hu, Yang Yu, Yao Li, Yan Wang, Jia Li,<sup>\*</sup> Xiao-Peng He,<sup>\*</sup> and He Tian



Cite This: *J. Am. Chem. Soc.* 2020, 142, 18005–18013



Read Online



### 个人简介

2002年9月—2006年6月，华东理工大学，化学与分子工程学院，本科

2006年9月—2011年6月，华东理工大学，药学院，硕博连读

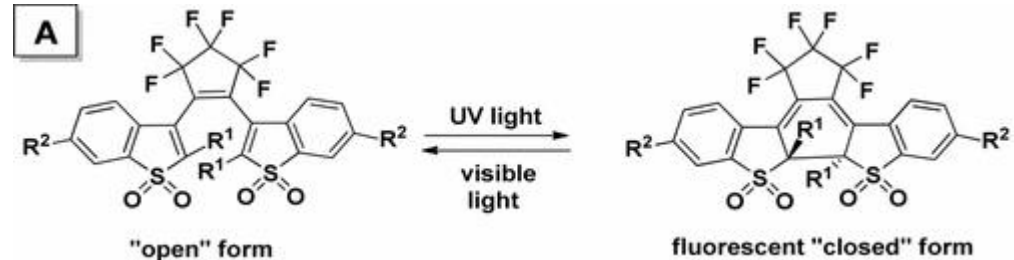
2011年7月—2013年6月，华东理工大学，化学与分子工程学院，博士后

### 研究领域

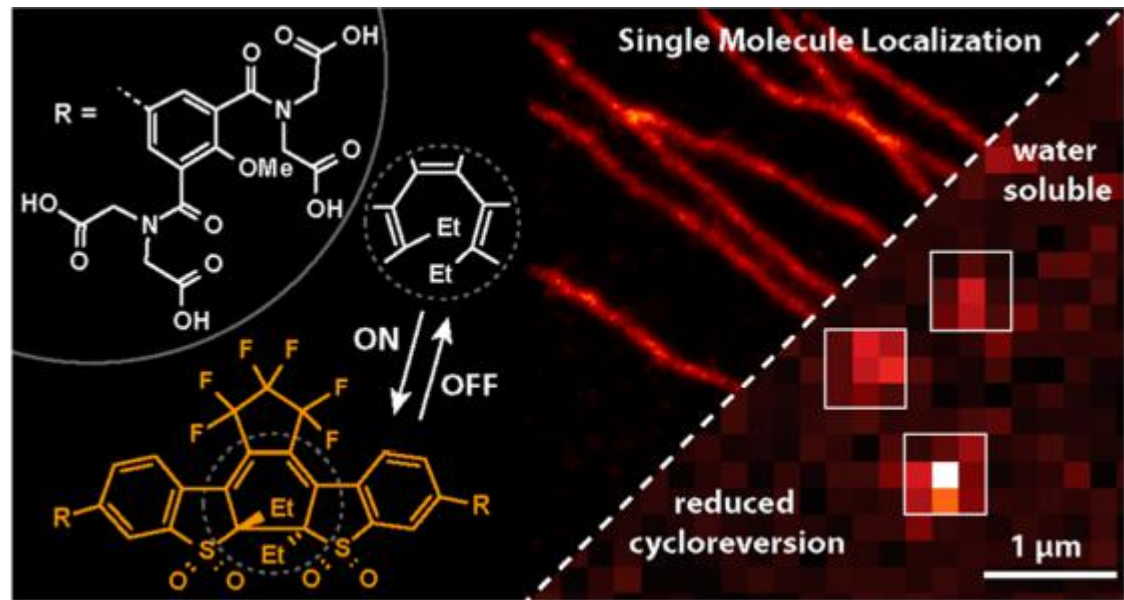
医学为导向的化学生物学研究，主要围绕以下两方面开展研究：

- 1) 靶向重要生命与疾病过程的生物基（糖、多肽等）分子探针和超分子材料构建。
- 2) 临床医学为导向的新型光学体外诊断试剂盒研发。

# Introduction

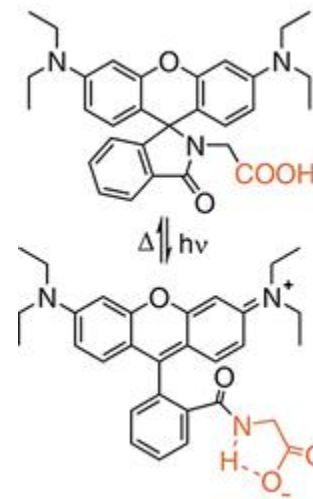


Sulfone Derivatives of Diarylethenes (DAEs)

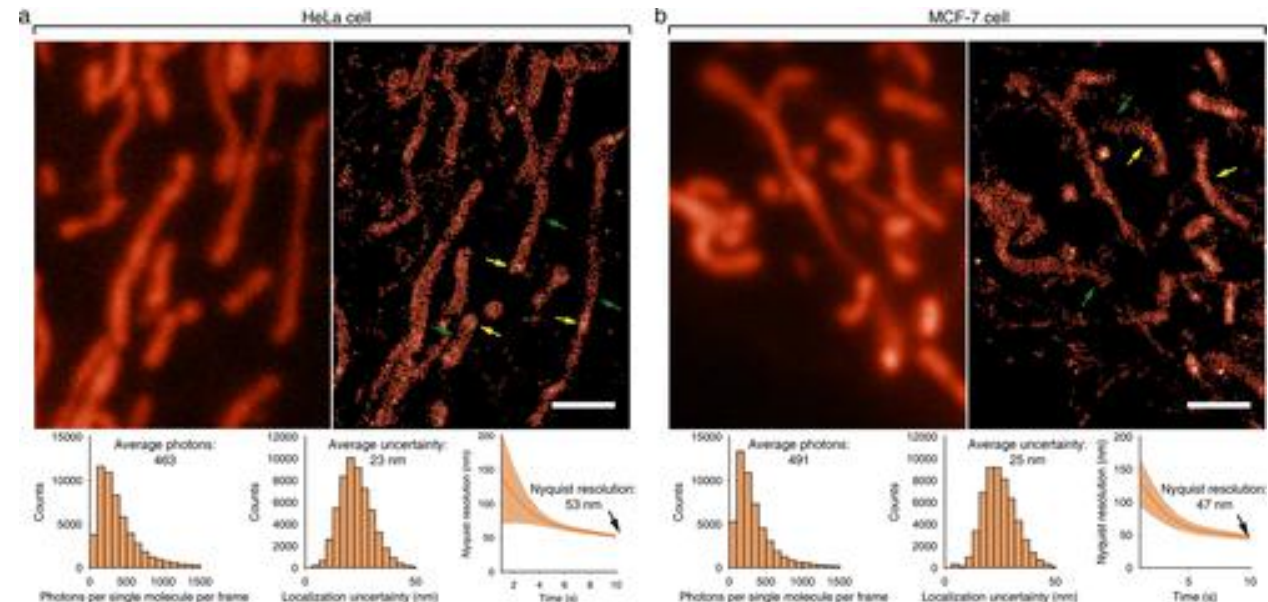


Superresolution images (STORM) of tubulin in Vero cells

J. Am. Chem. Soc. 2017, 139, 6611.



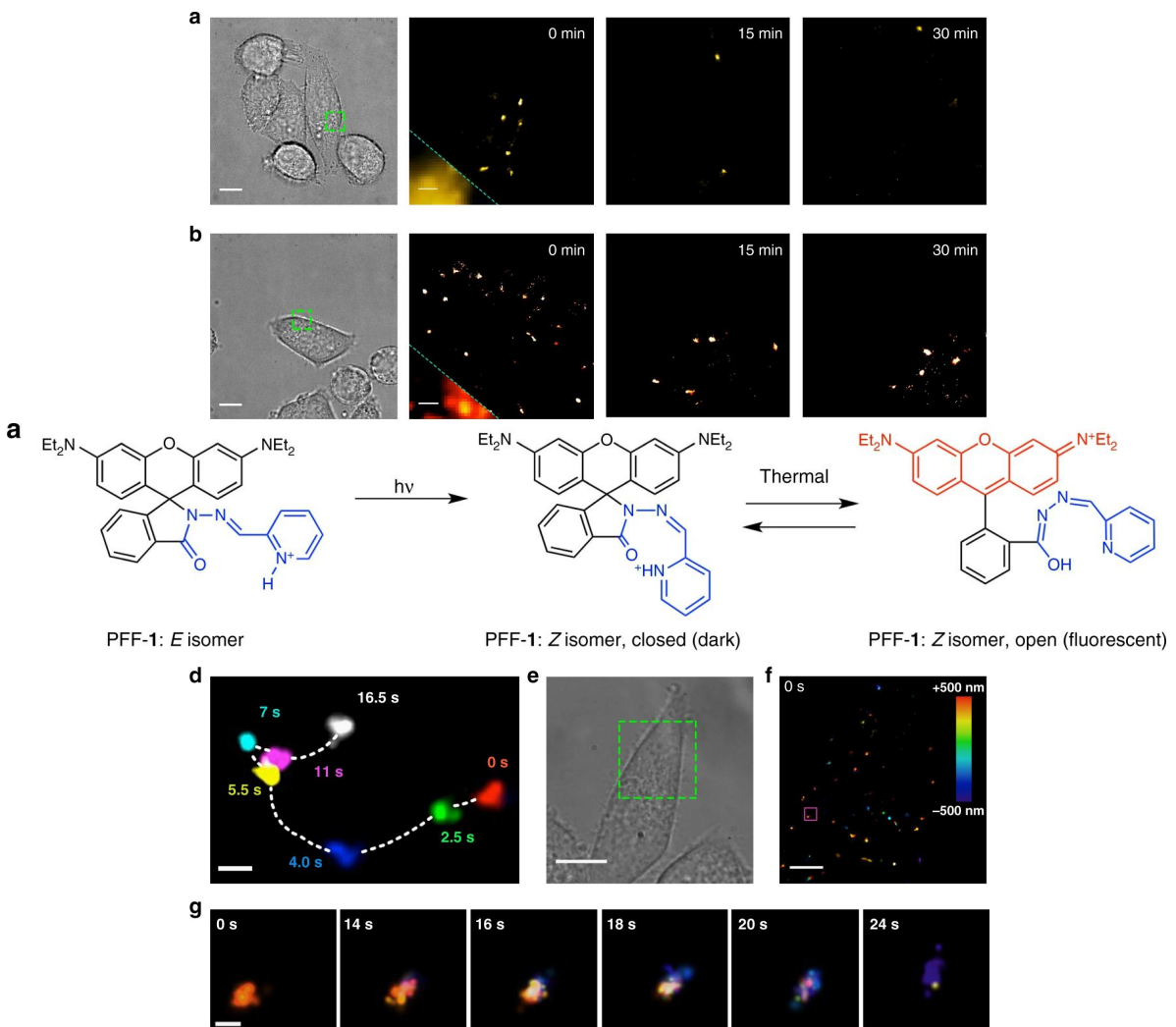
Rhodamine derivatives



Super-resolution imaging of mitochondria-enriched regions in live HeLa (panel a) and MCF-7 (panel b) cells stained with Rh-Gly

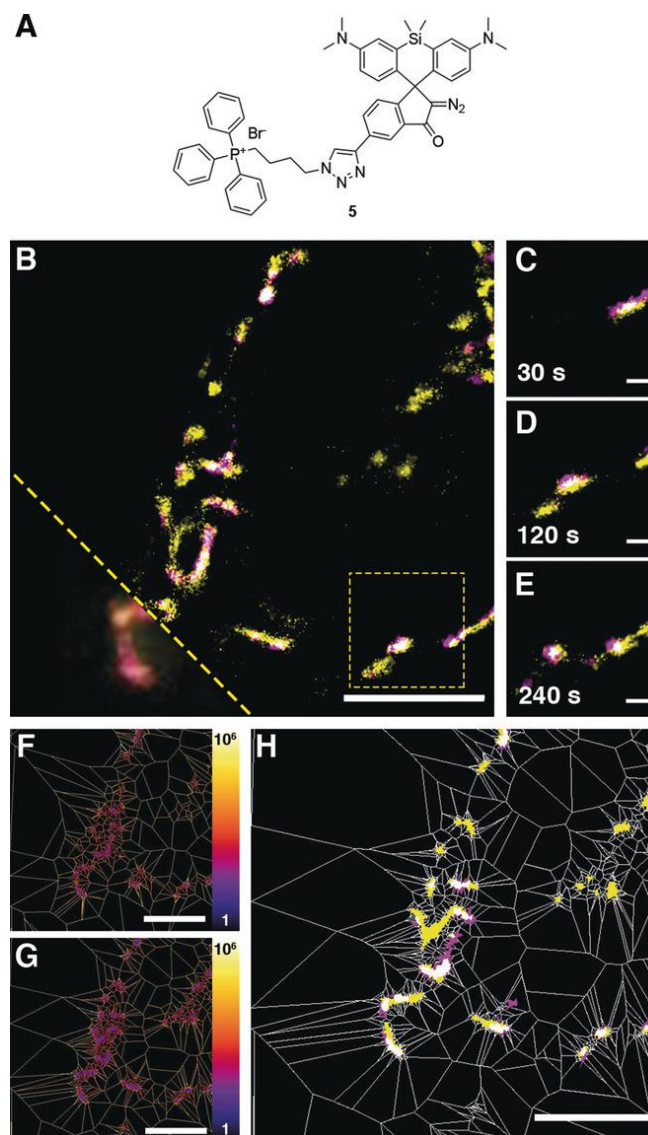
J. Am. Chem. Soc. 2019, 141, 6527.

# Introduction



Time-lapse, 2D and 3D SMLM of lysosomes in live HeLa cells using PFF-1.

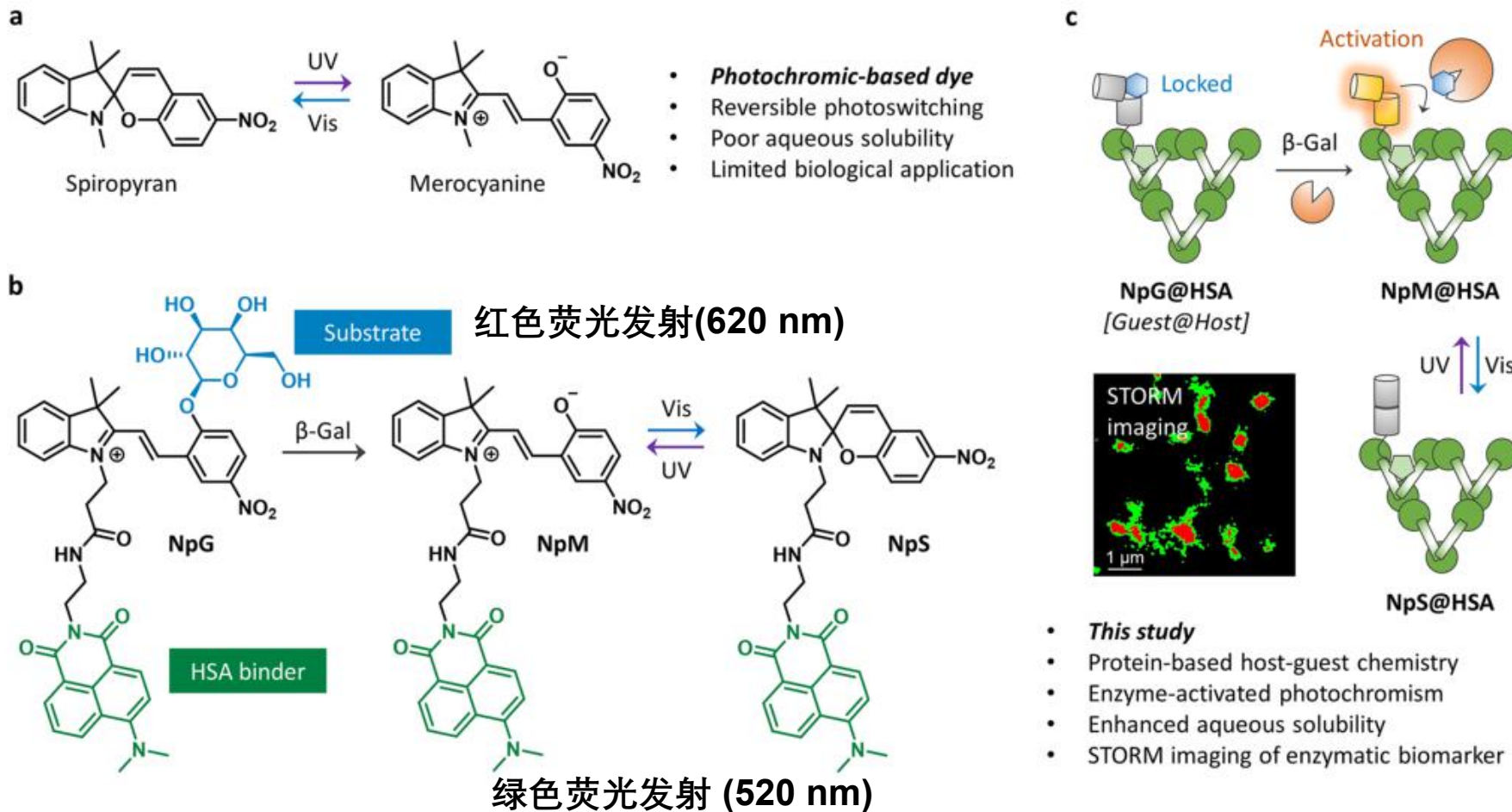
Nature communications, 2019, 10 (1): 1-10.



STORM super-resolution microscopy of nitroreductase activity in live HEK 293 cells.

Angew. Chem. Int. Ed., 2019, 58, 11474.

# Introduction



**Scheme 1.** (a) Photochromic Spiropyran Dye for Reversible Photoswitching Applications<sup>31</sup> and (b) Structure and (c) Fluorescence “Turn-On” Mechanism of NpG@HSA for the Monitoring of  $\beta\text{-Gal}$  with Super-resolution Imaging Technique STORM

# Introduction

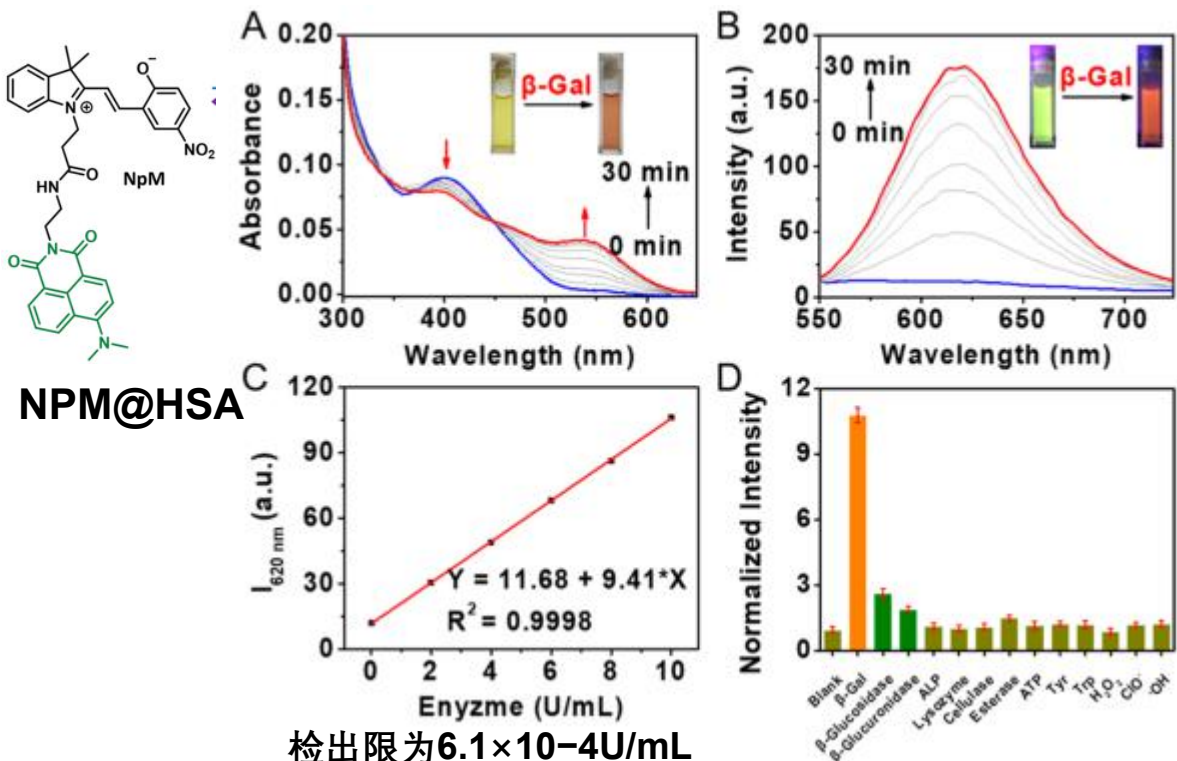


Figure 1. (A) Time-dependent UV-vis absorption and (B) fluorescence emission changes over time for **NpG@HSA** ( $5 \mu\text{M}$ ) after incubation with  $\beta\text{-Gal}$  ( $10 \text{ U/mL}$ ) in PBS buffer ( $10 \text{ mM}$ , pH  $7.4$ ,  $0.5\%$  DMSO), respectively. Blue line,  $0 \text{ min}$ ; red line,  $30 \text{ min}$ . (C) Plots and linear fit of the fluorescence intensity of **NpM@HSA** at  $620 \text{ nm}$  as a function of  $\beta\text{-Gal}$  concentration ( $0\text{--}10 \text{ U/mL}$ ) after  $30 \text{ min}$  of incubation. (D) Fluorescence change in **NpG@HSA** at  $620 \text{ nm}$  with various biomolecules or enzymes after incubation for  $30 \text{ min}$  in PBS buffer ( $10 \text{ mM}$ , pH  $7.4$ ,  $0.5\%$  DMSO).  $\text{H}_2\text{O}_2$  ( $0.1 \text{ mM}$ ),  $\text{ClO}^-$  ( $0.1 \text{ mM}$ ),  $\cdot\text{OH}$  ( $0.1 \text{ mM}$ ), ATP ( $0.1 \text{ mM}$ ), tyrosine (Tyr,  $0.1 \text{ mM}$ ), tryptophan (Trp,  $0.1 \text{ mM}$ ),  $\beta\text{-glucosidase}$  ( $10 \text{ U/mL}$ ),  $\beta\text{-glucuronidase}$  ( $10 \text{ U/mL}$ ), ALP ( $10 \text{ U/mL}$ ), lysozyme ( $10 \text{ U/mL}$ ), cellulase ( $10 \text{ U/mL}$ ), and esterase ( $10 \text{ U/mL}$ ). All emissions were produced upon excitation at  $530 \text{ nm}$ .

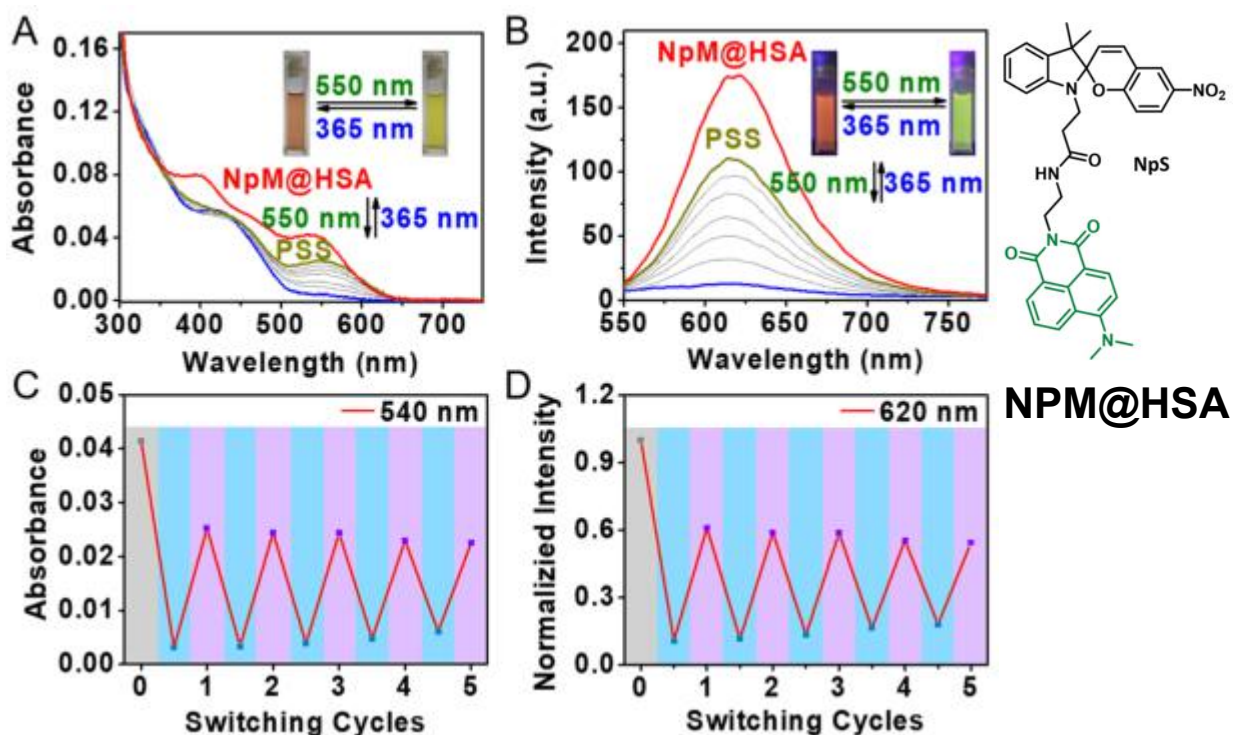
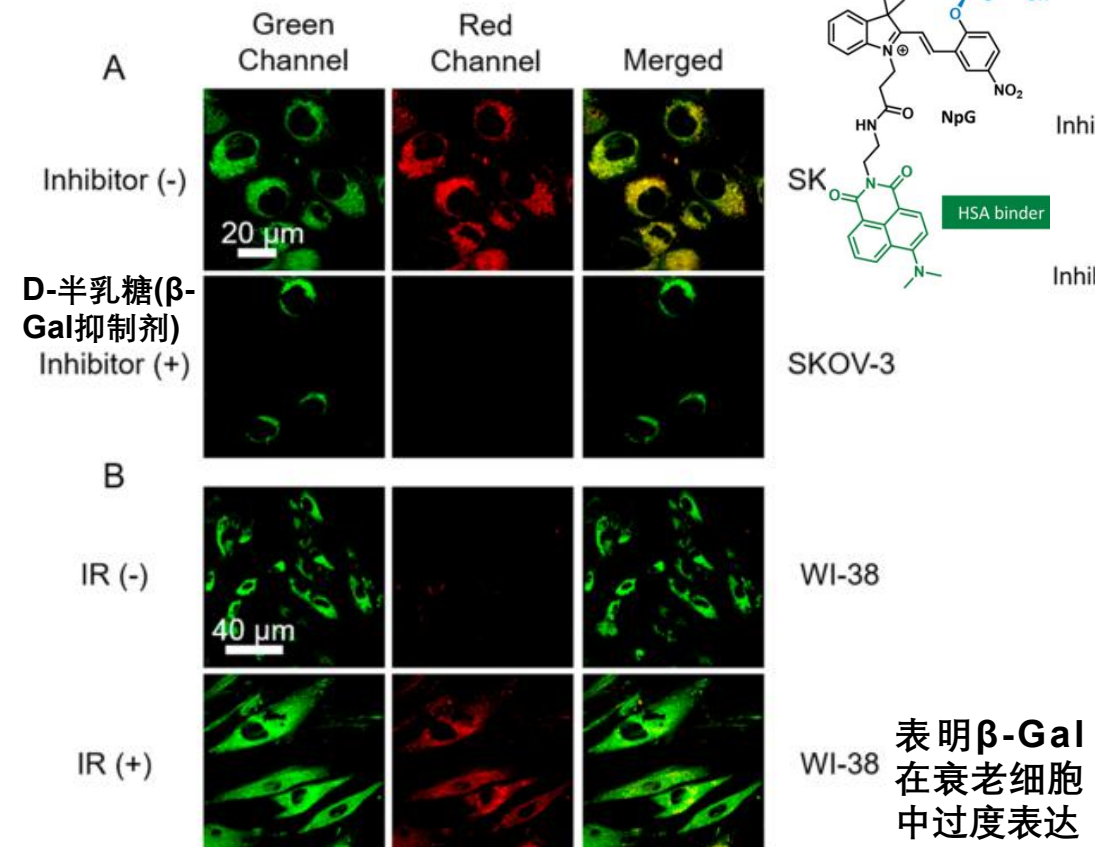
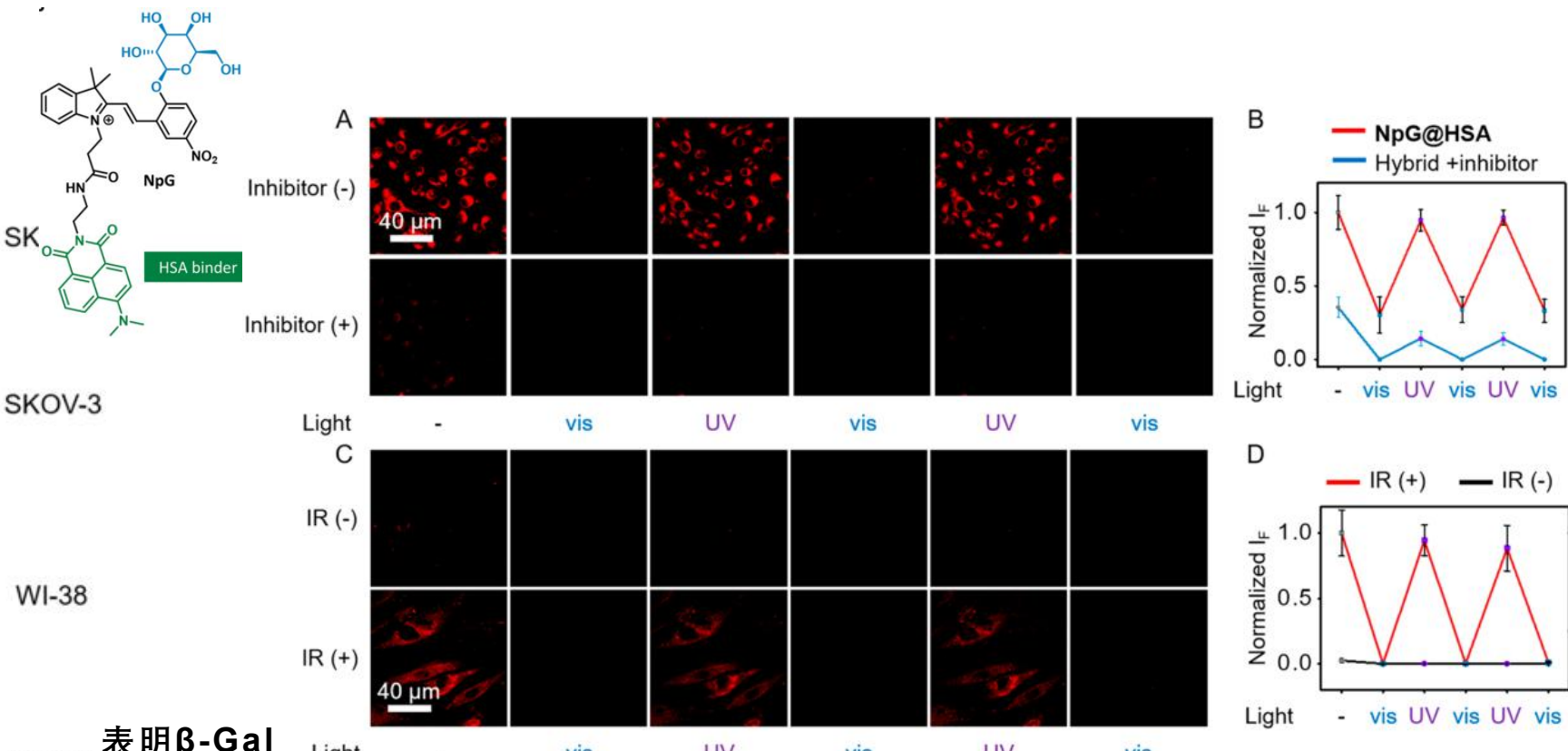


Figure 2. (A) UV-vis absorption and (B) fluorescence emission changes of **NpM@HSA** upon irradiation with alternate visible light ( $550 \text{ nm}$ ,  $150 \text{ mW cm}^{-2}$ ,  $1 \text{ min}$ ) and UV light ( $365 \text{ nm}$ ,  $160 \text{ mW cm}^{-2}$ ,  $5 \text{ min}$ ), respectively. Red line, **NpM@HSA**; blue line, upon irradiation with  $550 \text{ nm}$  visible light for  $1 \text{ min}$  (mainly in the spiropyran isomer); yellow line, photostationary state (PSS) after irradiation with UV light for  $5 \text{ min}$ . (C) Photofatigue resistance performances of the UV-vis absorption at  $540 \text{ nm}$  and (D) fluorescence emission at  $620 \text{ nm}$  of **NpM@HSA** upon irradiation with alternate visible light ( $550 \text{ nm}$ ,  $150 \text{ mW cm}^{-2}$ ,  $1 \text{ min}$ ) and UV light ( $365 \text{ nm}$ ,  $160 \text{ mW cm}^{-2}$ ,  $5 \text{ min}$ ), respectively. All emissions were produced upon excitation at  $530 \text{ nm}$ .

# Introduction



**Figure 3.**  $\beta$ -Gal-activated fluorescence OFF-ON imaging in live cells of NpG@HSA. (A) Confocal imaging of SKOV-3 cells incubated with NpG@HSA ( $20 \mu\text{M}$ ) for 40 min with or without preincubated D-galactose ( $1 \text{ mM}$ ) as an inhibitor. (B) Confocal imaging of WI-38 cells incubated with NpG@HSA ( $20 \mu\text{M}$ ) for 40 min with or without treatment by ionizing radiation (IR, 12 Gy). Green channel: Ex/Em =  $488/530-540 \text{ nm}$ . Red channel: Ex/Em =  $559/600-620 \text{ nm}$ .



**Figure 4.** (A) Fluorescence imaging of SKOV-3 cells incubated with NpG@HSA ( $20 \mu\text{M}$ ) for 40 min in the absence (line 1) and presence of D-galactose ( $1 \text{ mM}$ , line 2) upon alternate irradiation with UV and visible light. (B) Fluorescence quantification of the images shown in panel a with photoswitching cycles. (C) Fluorescence imaging of endogenous  $\beta$ -Gal in WI-38 cells with or without ionizing irradiation after incubation with NpG@HSA ( $20 \mu\text{M}$ ) for 40 min. (D) Fluorescence quantification of the images shown in panel c with photoswitching cycles. Red channel: Ex/Em =  $559/600-620 \text{ nm}$ . For photoswitching excitation, UV,  $405 \text{ nm}$ , 30 s; vis,  $559 \text{ nm}$ , 10 min.

# ➤ Introduction

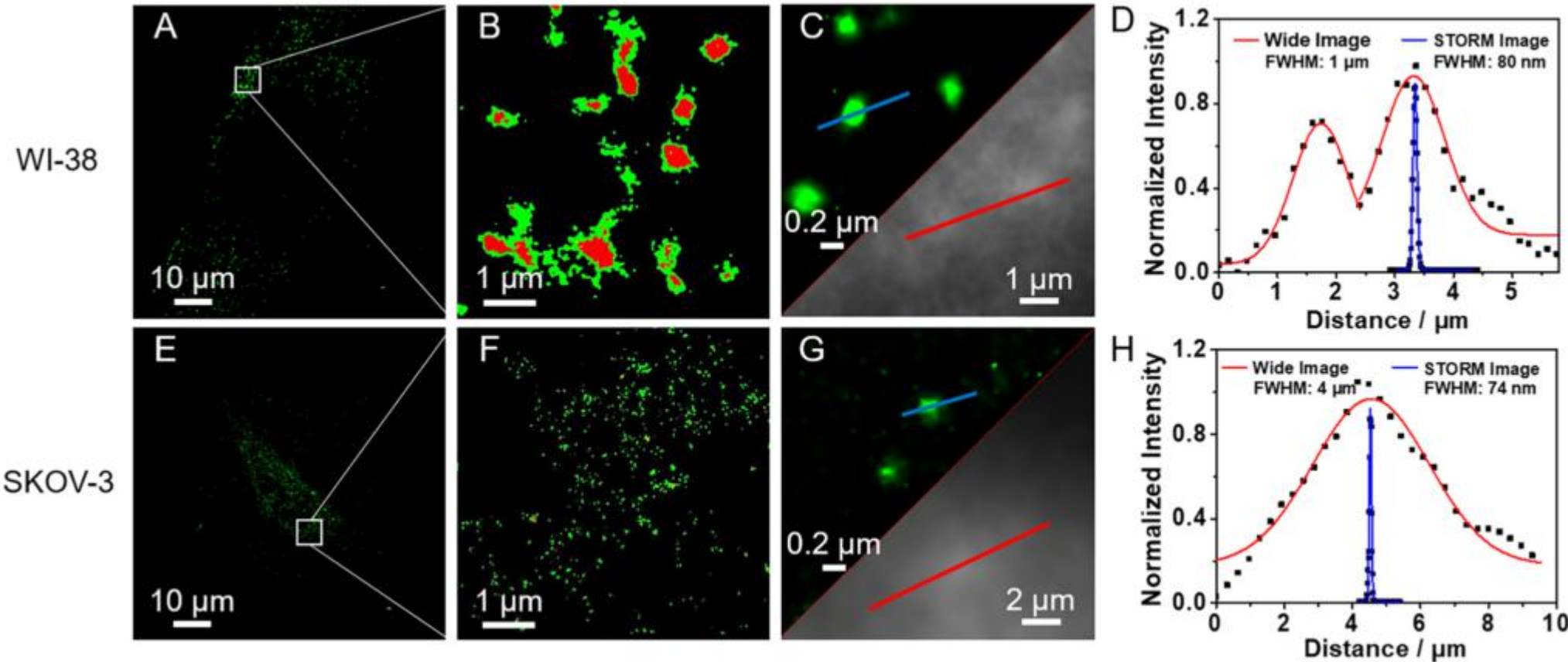


**Figure 5.** Subcellular imaging of  $\beta$ -galactosidase in cancerous and senescent cells using STORM. (A) Super-resolution images (STORM) of senescent WI-38 cells and (E) SKOV-3 cells incubated with NpG@HSA (20  $\mu$ M), respectively. (B) Close-up images of panel a reconstructed from 16 000 frames. Scale bar: 1  $\mu$ m. (F) Close-up images of panel e reconstructed from 16 000 frames. Scale bar: 1  $\mu$ m. (C, D) Calculation of fwhm in WI-38 cells of the STORM image and wide image, respectively. (G, H) Calculation of fwhm in SKOV-3 cells of the STORM image and wide image, respectively.

# ➤ Introduction

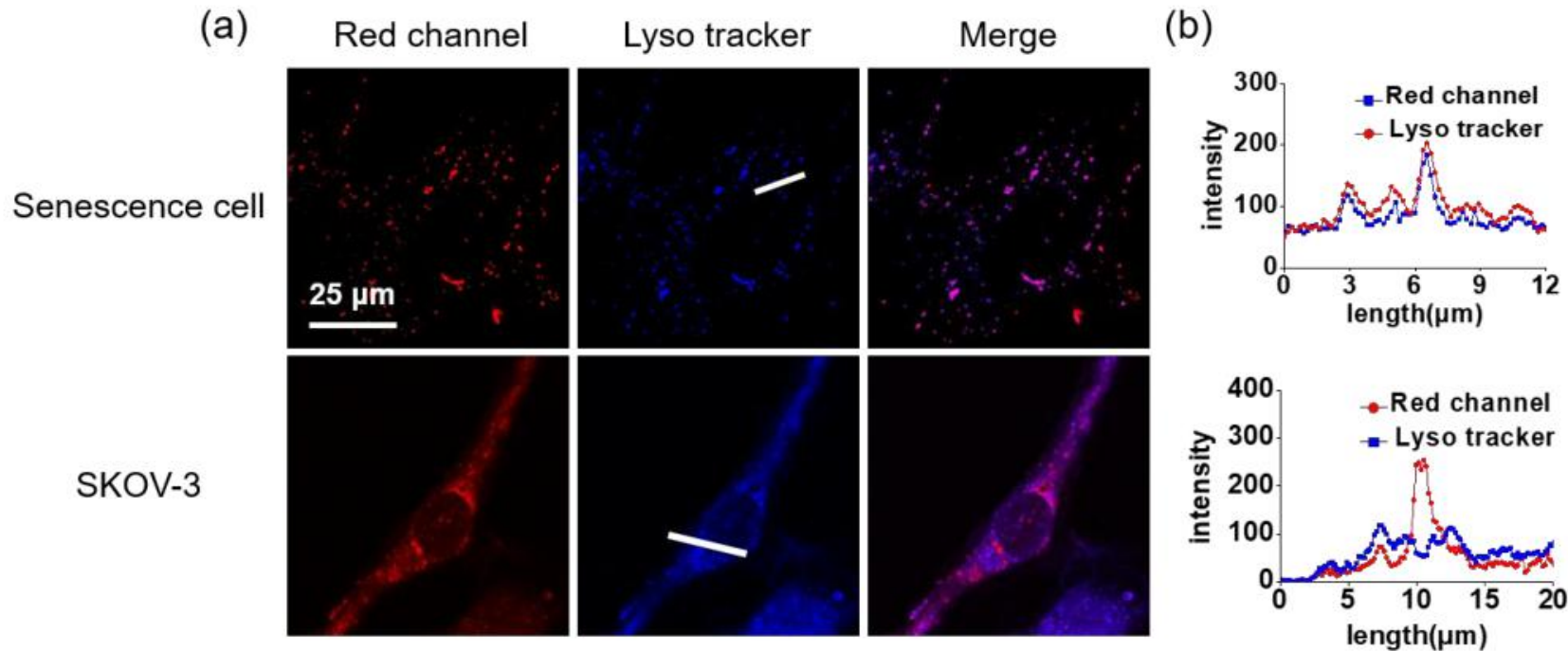


**Figure S10.** (A) Fluorescence co-localization experiments of **NpG@HSA** (20  $\mu$ M) with Lysotracker® Deep Red (500 nM) in senescence cells ( $H_2O_2$ -induced) and SKOV-3 cells. (B) Fluorescence quantification of **NpG@HSA** (20  $\mu$ M) with Lysotracker® Deep Red (500 nM) of a selected section (the white line in “Lysotracker” panel) in senescence cells (Top) and SKOV-3 cells (Bottom). **NpG@HSA** red channel excitation: 559 nm, emission: 600-620 nm; Lysotracker channel excitation: 633nm, emission: 650-670 nm.

用Lysotracker进行的共定位实验得到了很高的 Pearson's correlation efficient (0.955)，表明在衰老细胞中NpG@HSA主要定位在溶酶体。

SKOV-3细胞的Pearson's correlation efficient很低(0.496)，进一步表明了NpG@HSA在胞浆内随机分布